Biogeosciences, 23, 6431–6445, 2026
https://doi.org/10.5194/bg-23-6431-2026
© Author(s) 2026. This work is distributed under
the Creative Commons Attribution 4.0 License.

Biogeosciences Open Access EGU

Stoichiometric deviation and regulatory mechanisms of AOU–nutrient ratio in the oligotrophic Northwest Pacific Ocean

Detong Tian[1], Xuegang Li[2,3], Jinming Song[2,3], Yunping Xu[1], Feng Zhao[2], Jun Ma[2,3], Shanshan Liu[2,3], Muhammad Inayat Ullah Khan[1], and Weichao Wu[1,4]

[1]College of Oceanography and Ecological Science, Shanghai Ocean University, Shanghai, 201306, China
[2]Institute of Oceanology, Chinese Academy of Sciences, Qingdao 266000, China
[3]Laboratory for Marine Ecology and Environmental Science, Qingdao Marine Science and Technology Center, Qingdao 266237, China
[4]International Research Center for Marine Biosciences at Shanghai Ocean University, Ministry of Science and Technology, China

Correspondence: Xuegang Li (lixuegang@qdio.ac.cn) and Weichao Wu (wcwu@shou.edu.cn)

Received: 22 May 2026 – Discussion started: 12 June 2026
Revised: 1 September 2026 – Accepted: 7 September 2026 – Published: 16 September 2026

Abstract. In oligotrophic oceans, the stoichiometric ratios of apparent oxygen utilization (AOU) to nutrients often deviate from the classical Redfield ratio, yet the mechanisms remain poorly constrained. Contrary to the commonly held view that these ratios are typically elevated, we found that the mean ratios of AOU to dissolved inorganic nitrogen (DIN) and AOU to dissolved inorganic phosphorus (DIP) over the upper 2000 m of the oligotrophic Northwest Pacific are only 6.28 and 86.79, respectively, both below the classical values of 8.6 and 138. Strong stratification indicates that physical mixing alone cannot explain these integrated patterns, while depth-resolved regressions further reveal distinct controls among water layers. In upper waters, nutrient limitation promotes phytoplankton to produce TEPs with high C : N ratios, decoupling carbon fixation from nutrient assimilation, a process in which *Pelagibacter* may play a key role in recycling small organic molecules. In intermediate waters, preferential degradation of low C : N compounds within sinking organic matter enhances nutrient regeneration relative to oxygen consumption. In deep water, AOU / nutrient relationships are not statistically significant, indicating that oxygen consumption and nutrient accumulation become increasingly decoupled; this decoupling is likely influenced by *Alteromonas* activity in polymer degradation and phosphorus mobilization, alongside archaeal nitrification. These findings suggest that biogeochemical models should account for such biological feedbacks to improve predictions of ocean carbon export and nutrient cycling under future climate scenarios.

1 Introduction

The ocean is the largest active reservoir of carbon and nutrients on Earth, and its internal biogeochemical cycles are crucial for sustaining the productivity of marine ecosystems (Friedlingstein et al., 2025). The supply of nutrients such as nitrogen and phosphorus directly affects marine primary productivity, and the regeneration of these nutrients is closely coupled with the production, export, and burial of organic carbon, thereby collectively regulating the intensity of the marine biological pump and the global carbon cycle (Longhurst and Glen Harrison, 1989; Smith et al., 2008). Apparent oxygen utilization (AOU) serves as a key link between surface photosynthesis and deep-water heterotrophic respiration and reflects the amount of dissolved oxygen (DO) consumed by respiration during the transport and sedimentation of organic matter in waters (Ito et al., 2004; Sulpis et al., 2023). Classical Redfield stoichiometry establishes a proportional relationship between AOU, nutrient regeneration, and the accumulation of dissolved inorganic carbon (DIC), which has led to the widespread use of AOU / nutrient ratios, such as AOU / dissolved inorganic nitrogen (DIN) and AOU / dissolved inorganic phosphorus (DIP) ratios, to infer

the elemental composition of degraded organic matter (Tanioka and Matsumoto, 2020). However, the relationships between AOU and nutrients in marine environments often deviate from classical stoichiometry, highlighting the presence of complex physical and biogeochemical regulatory mechanisms.

Numerous observations indicate that the AOU / nutrient ratios in many oceanic regions generally exceed the classical Redfield ratio (i.e., AOU / DIN = 8.6 and AOU / DIP = 138) (Delaigue et al., 2024; Anderson and Sarmiento, 1994). This pattern is particularly evident in highly stratified oligotrophic waters, where the degradation rates of suspended and dissolved organic matter are slow, and spatiotemporal decoupling between production and remineralization occurs (Dai et al., 2023). In these areas, some organic matter may migrate horizontally before settling or undergo multiple cycles within surface waters. Simultaneously, the C : N ratio of nitrogen sources supplied by nitrogen-fixing organisms is generally higher than the Redfield value, resulting in greater oxygen consumption per unit of nitrogen regenerated during degradation (Körtzinger et al., 2001; Singh et al., 2015). Furthermore, DIC generated by shallow respiration as a result of organic matter degradation by heterotrophic organisms may precede nutrient regeneration, and potential non-photosynthetic oxidation processes also contribute to elevated AOU / nutrient ratios in oligotrophic regions (Calleja et al., 2019). In contrast, in well-mixed marginal shelf seas where organic matter sources are complex, strong physical agitation disrupts the coupling between AOU and nutrients. This leads to highly scattered ratios that are systematically lower than the Redfield values, reflecting the influence of physical processes on biogeochemical signals (Zhu et al., 2025). Because strong mixing can obscure local relationships between AOU and nutrient, residual nutrient diagnostics can be particularly useful in stratified oligotrophic systems, where water masses are more clearly resolved. Residual preformed total oxidised nitrogen ($rPreNO_x$) and residual preformed phosphate ($rPrePO_4$) can be used to evaluate whether measured nutrient inventories are consistent with the regeneration predicted from AOU under parameterized dissolved organic matter (DOM) and particulate organic matter (POM) remineralization (Letscher and Villareal, 2018). Although dependent on the chosen parameters, these residuals can identify deviations from the preset relationship.

The Tropical Northwest Pacific (TNWP) is a key region for global ocean circulation and biogeochemical cycling, featuring the Western Pacific Warm Pool (WPWP), the world's largest warm-water body, where high sea surface temperatures and strong stratification create an extensive oligotrophic zone (Radenac et al., 2013). Complex ocean circulation systems converge here, forming vertically layered water masses that significantly influence nutrient supply, organic matter production, transport, and transformation (Hu et al., 2015; Sun et al., 2008; Jian et al., 2022). Numerous studies have characterized the macroscopic distribution of nutrients in this region (Ma et al., 2021a) as well as the vertical degradation patterns of particulate organic carbon (POC) (Tian et al., 2025). However, POC is a complex mixture comprising components with diverse chemical compositions and sources, and its various components differ significantly in terms of bioavailability and their roles in the carbon cycle (Kharbush et al., 2020). Therefore, the roles of specific functional particulate components within POC in regional organic matter transport and transformation have gradually become a focus of research in recent years (Digernes et al., 2025). Among these components, transparent exopolymer particles (TEPs) are a class of polysaccharide colloid primarily secreted by phytoplankton, characterized by a high C : N ratio (Engel and Passow, 2001). Although their absolute concentrations are often low in oligotrophic oceans, TEP can constitute a substantial fraction of the small POC pool and can be abundant relative to the low phytoplankton biomass (Kodama et al., 2014). Meanwhile, regional differences in microbial community structure and function are considered to directly affect organic matter degradation and nutrient regeneration processes, thereby regulating the stoichiometry of deep nutrient regeneration and efficiency of the carbon cycle (Guo et al., 2023; Saavedra et al., 2025). However, although numerous studies have revealed several biogeochemical characteristics of this region from different perspectives, our overall understanding remains relatively fragmented. In particular, the stoichiometric characteristics of organic matter degradation in waters of varying sources and ages, as well as the mechanisms driving deviations from the Redfield ratios, remain unclear. Additionally, there is a lack of systematic field evidence regarding how microbial metabolic strategies influence the coupled cycles of carbon, nitrogen, and phosphorus.

In the present study, suspended POM and water samples were collected from six water columns within and around the core area of the TNWP Warm Pool. The aim was to elucidate the coupled mechanism linking physical stratification, organic matter transformation, nutrient regeneration, and microbial regulation in the oligotrophic waters of the western Pacific by integrating multiple biogeochemical and microbial parameters.

2 Materials and Methods

2.1 Research area and sample collection

From February to April 2022, a research cruise was conducted aboard the R/V *Kexue* (voyage NORC2021-09) in the TNWP Warm Pool. During the survey, a total of six sampling stations were set up: EQ-6, E142-3, E142-7, E142-11, E142-13, and E142-19 (Fig. 1).

Seawater samples were collected from 16 depths (5, 50, 100, 150, 200, 300, 400, 500, 600, 800, 1000, 1200, 1400, 1600, 1800, and 2000 m) using 12 L Niskin bottles

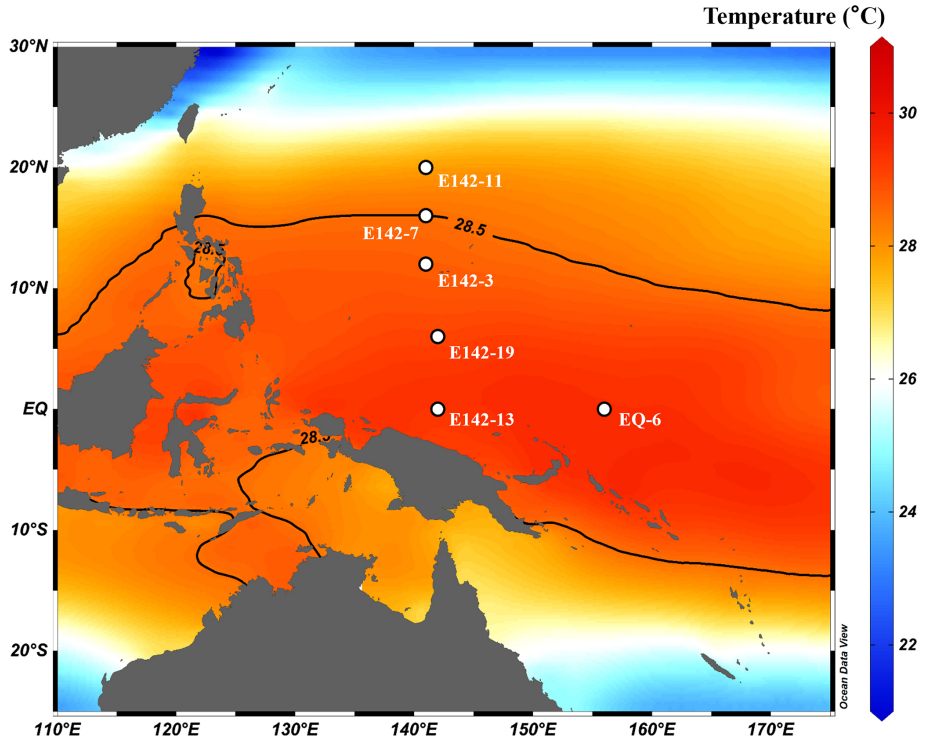

Figure 1. Study area and sampling stations in the Tropical Northwest Pacific. The sampling area is located in the Western Pacific Warm Pool, and the 28.5 °C isotherms are shown as black lines. Credit: Schlitzer (2026).

(KC-Denmark, Denmark) mounted on a shipboard CTD rosette (Conductivity-Temperature-Depth, Sea-bird SBE911, United States). After seawater collection, DO samples were first aliquoted and fixed in 50 mL amber glass bottles. Then, the seawater was filtered through pre-combusted and acid-washed GF/F glass fiber filters (0.7 µm pore size, Whatman; 450 °C for 4 h, 0.5 M HCl for 24 h), followed by the collection of nutrient and DIC samples. Samples for nutrient determination were aliquoted into 250 mL high-density polyethylene bottles, amended with chloroform (approximately 1 : 500, v/v) to suppress biological activity during delayed analysis, and stored frozen at −20 °C before measurement (Ma et al., 2023). Samples for DIC analysis were collected in 50 mL airtight glass bottles. After overflow, 1 mL of the water sample was withdrawn and the remaining sample was poisoned with saturated mercuric chloride solution to suppress biological activity. The samples were stored at 4 °C until analysis.

Suspended particulate samples for POC analysis were collected by filtering 2–4 L of seawater through pre-combusted and acid-washed GF/F glass fiber filters (0.7 µm pore size, Whatman; 450 °C for 4 h, 0.5 M HCl for 24 h). Samples were stored at −20 °C until measurement. TEP samples were collected by filtering 1–4 L of seawater through polycarbonate filters (0.45 µm pore size, Whatman) under a vacuum of 170 mmHg. The retained particles were stained with 0.5–1 mL of a 400 mg L^{-1} Alcian Blue solution (Sigma-Aldrich, USA) for 5–10 s, prepared in Milli Q water and acidified to pH 2.5 with glacial acetic acid. The filters were then rinsed with 5 mL of MilliQ water, and stored at −20 °C until measurement (three replicate samples were collected at each depth). Samples for chlorophyll *a* (Chl *a*) determination were collected from five depths between 5 and 200 m. First, 2 L of seawater samples were filtered through a 200 µm mesh to remove zooplankton and then filtered onto a 0.7 µm GF/F glass fiber membrane (Whatman; 450 °C for 4 h, 0.5 M HCl for 24 h). The filters were then stored at −80 °C until analysis in the shore-based laboratory. Seawater samples (20 L) for microbial community analysis were similarly pre-filtered through a 200 µm mesh and then filtered through a 0.22 µm mixed cellulose ester (MCE) membrane. The filtered samples were immediately transferred to cryovials, supplemented with RNA Later stabiliser (Qiagen, Germany), and stored at −80 °C.

2.2 Chemical analysis

2.2.1 Temperature, salinity, DO, and Chl *a*

For each station, temperature, salinity, and DO were measured in situ using a shipboard CTD. Simultaneously, discrete DO samples were fixed and titrated according to the Winkler method with an accuracy of 0.22 µmol L^{-1} (Bryan et al., 1976). These discrete DO samples were used to calibrate the DO concentration data obtained from the CTD sensor. Chl *a* concentrations were determined by acetone extraction.

Filters containing Chl *a* were extracted with 90 % acetone for 14 h, and the Chl *a* concentration was then measured using a Turner fluorometer (Turner Designs, United States) (Ma et al., 2020).

2.2.2 Nutrients

Phosphate (PO_4-P, as dissolved inorganic phosphorus, DIP), nitrate (NO_3-N), nitrite (NO_2-N), ammonium (NH_4-N), and silicate (SiO_3-Si, as dissolved inorganic silicon, DSi) concentrations were determined using a QuAAtro nutrient analyzer (SEAL, Germany). The limits of detection for PO_4-P, NO_3-N, NO_2-N, NH_4-N and SiO_3-Si were 0.01, 0.02, 0.01, 0.01 and 0.01 µmol L^{-1}, respectively. The DIN concentration was the sum of the concentrations of NO_3-N, NO_2-N, and NH_4-N.

2.2.3 POC and DIC

The particulate filters were freeze-dried at −50 °C for 24 h. After drying, the filters were acid-fumed with concentrated hydrochloric acid for 12 h to remove inorganic carbonates and then dried at < 60 °C. The dried membrane samples were wrapped in a tin boat for subsequent analysis. The pretreated samples were analyzed for POC concentration using an elemental analyzer (Thermo Fisher Scientific Flash EA 1112, United States). Carbon quantification was calibrated using standard reference materials, including USGS64 (C % = 31.97 %, Indiana University), USGS40 (C % = 40.8 %, U.S. Geological Survey), and Urea #2a (C % = 20 %, Indiana University), which were also used to monitor instrument performance (Ma et al., 2021b).

DIC concentrations were determined using an Apollo SciTech AS-C3 analyzer (United States) with an analytical precision of ±0.1 % (Ma et al., 2020). Calibration was performed using certified reference material (batch 144, 2031.53 ± 0.62 µmol L^{-1}) provided by the Scripps Institution of Oceanography (University of California, San Diego).

2.2.4 TEP

In the shore-based laboratory, the TEP filters were transferred to a 10 mL amber glass bottle, and 6 mL of 80 % (14.4 M) sulfuric acid solution was added for 10 h with periodic gentle mixing. The absorbance was then measured at 787 nm using a spectrophotometer (UV-1600, Shimadzu). The absorbance was converted to xanthan gum equivalents (Xeq) weight using a xanthan gum calibration curve prepared independently in our laboratory following the updated procedure of Bittar et al. (2018) (Fig. S1 in the Supplement). Details of the calibration procedure are provided in Sect. S1 in the Supplement.

2.2.5 Relative abundance of microorganisms

DNA was extracted from the filters using the All-Prep DNA/RNA Mini Kit (Qiagen, Germany). 16S rDNA was amplified using a universal bacterial primer set, F515 (5′GTGCCAGCMGCCGCGG3′) and R907 (5′CCGTCAATTCMTTTRAGTTT3′). To reduce PCR bias, three replicate PCR reactions were performed for each sample. The amplicon libraries were sequenced using the Illumina NovaSeq platform (Novogene, China). During data processing, primers and low-quality reads were removed using VSEARCH (v. 2.15.2), and sequences were denoised using USEARCH (v. 10.0.240) to obtain an amplicon sequence variant (ASV) table. The amplicon sequence variants (ASVs) were then analyzed using VSEARCH (v. 2.15.2) against a reference database. The RDP database (v. 16) was used to annotate the ASV tables. The ASV tables were standardized by resampling to ensure that the data from each sample are at the same level of comparison. The number of sequences assigned to each ASV in each sample was normalized to its proportion of total reads to calculate the relative abundance of microbial taxa (Liu et al., 2024).

2.3 Calculation of $rPreNO_x$ and $rPrePO_4$

$rPreNO_x$ and $rPrePO_4$ were calculated using the modified formulation of Letscher and Villareal (2018), with parameter sensitivity evaluated following Smyth and Letscher (2023). For each observation, 9 calculations were performed using the prescribed DOM and POM parameter combinations. The arithmetic mean was used as the reported diagnostic value, whereas the minimum, maximum, and standard deviation describe sensitivity to the prescribed parameters. Full equations and parameter values are provided in Sect. S2.

2.4 Data Processing

Data processing was performed using OriginPro 2021 (v. 9.8.0.200). Depending on whether the variables follow a normal distribution, correlation analyses were performed using either Pearson's or Spearman's rho test (two-tailed, $\alpha = 0.05$), with $p < 0.05$ considered significant. The normality of the data was tested using the Kolmogorov-Smirnov test (two-tailed, $\alpha = 0.05$). The AOU / nutrient ratios were estimated via simple linear regression using the ordinary least squares method, where AOU served as the dependent variable and the nutrient (nitrate or dissolved inorganic phosphate) as the independent variable. The slope of the resulting regression line represents the AOU per mole of nutrient regenerated (Álvarez-Salgado et al., 2014).

Table 1. Characteristics of water masses in the study area.

Vertical Layer	Water Masses	Temperature (°C)	Salinity	γ_n (kg m^{-3})
Upper Water	NPTSW	27.99–29.45 −28.71	34.29–34.63 −34.45	21.62–22.58 −21.76
	ESW	29.28–29.87 −29.56	34.59–35.27 −35.01	21.44–22.76 −21.89
	SPSSW	19.62–26.64 −22.95	35.46–35.52 −35.51	22.93–25.95 −24.25
	NPSSW	18.76–27.04 −23.89	34.62–34.98 −34.8	22.59–24.99 −23.51
	NPSTMW	13.23–16.45 −15	34.42–34.68 −34.55	25.00–26.00 −25.67
Intermediate Water	NPIW	3.91–11.16 −7.36	34.12–34.58 −34.4	26.01–27.59 −26.99
	SPIW	5.47–12.43 −8.55	34.52–34.94 −34.65	26.00–27.40 −26.99
Deep Water	NPDW	2.05–4.63 −3.07	34.51–34.63 −34.58	27.41–27.92 −27.76

3 Results

3.1 Hydrological characteristics of the study area

Temperature-salinity (T-S) diagram and the vertical distribution of temperature, salinity, and γ_n indicate pronounced stratification in the water column. Eight distinct water masses were identified and subsequently categorized into upper, intermediate, and deep waters based on their hydrographic properties and vertical positions (Fig. 2a, Table 1) (Sun et al., 2008). γ_n increases with depth from approximately 21.6 to 27.7 kg m^{-3} (Fig. 2d), reflecting the transition from low-density tropical upper waters to high-density deep waters.

In the upper waters, tropical surface waters and subsurface waters dominate. The North Pacific Tropical Surface Water (NPTSW) and Equatorial Surface Water (ESW) lie at the warmest end of the T-S diagram, with temperatures ranging from approximately 28–30 °C, characteristics of the WPWP. Below the mixed layer, the North Pacific Subsurface Water (NPSSW) and South Pacific Subsurface Water (SPSSW) exhibit pronounced salinity maxima along the 23–25 kg m^{-3} isopycnals. Both water masses have temperatures lower than the overlying surface waters (approximately 19–27 °C). The salinity of the SPSSW is the highest in the upper ocean (mean 35.51), while the NPSSW is slightly fresher (mean 34.80) (Fig. 2a, Table 1). The North Pacific Subtropical Mode Water (NPSTMW) constituted the lower part of the upper water, with stable physicochemical properties. The intermediate waters comprised the North Pacific Intermediate Water (NPIW) and South Pacific Intermediate Water (SPIW). The NPIW is characterized by low salinity (mean 34.12), exhibiting a salinity minimum in the T-S diagram (Fig. 2a). The SPIW has slightly higher temperature and salinity relative to NPIW. Its γ_n value largely overlaps with those of the NPIW, suggesting substantial mixing between the two within the study area. The deep water was represented by North Pacific Deep Water (NPDW), which had low temperatures, relatively uniform salinity, and high density (Fig. 2b–d, Table 1).

3.2 Vertical distribution of chemical parameters across water column

DIN, phosphate, and silicate concentrations were low in the upper waters and increased markedly with depth, reaching their maxima in the deep waters (Fig. 3a–c). The ensemble mean rPreNO$_x$ and rPrePO$_4$ values were positive in the upper waters and generally increased with depth, reaching their highest values in the deep waters (Fig. 3d, e). Although the absolute magnitudes of the residuals varied among the 9 parameterizations, the main vertical pattern remained consistent across the parameter ensemble. The corresponding ranges and summary statistics are available in the public data set (Tian, 2026).

AOU and DIC showed broadly parallel vertical distributions, with low upper water values and marked increases into the intermediate and deep waters (Fig. 3f, h). In contrast, POC and TEP exhibit a distribution pattern that is nearly opposite to that of nutrients and DIC (Fig. 3g, h, i). TEP concentrations in the upper water ranged from 7.53 to 34.22 µg Xeq L^{-1} (mean 22.52 ± 8.54 µg Xeq L^{-1}), exceeding those

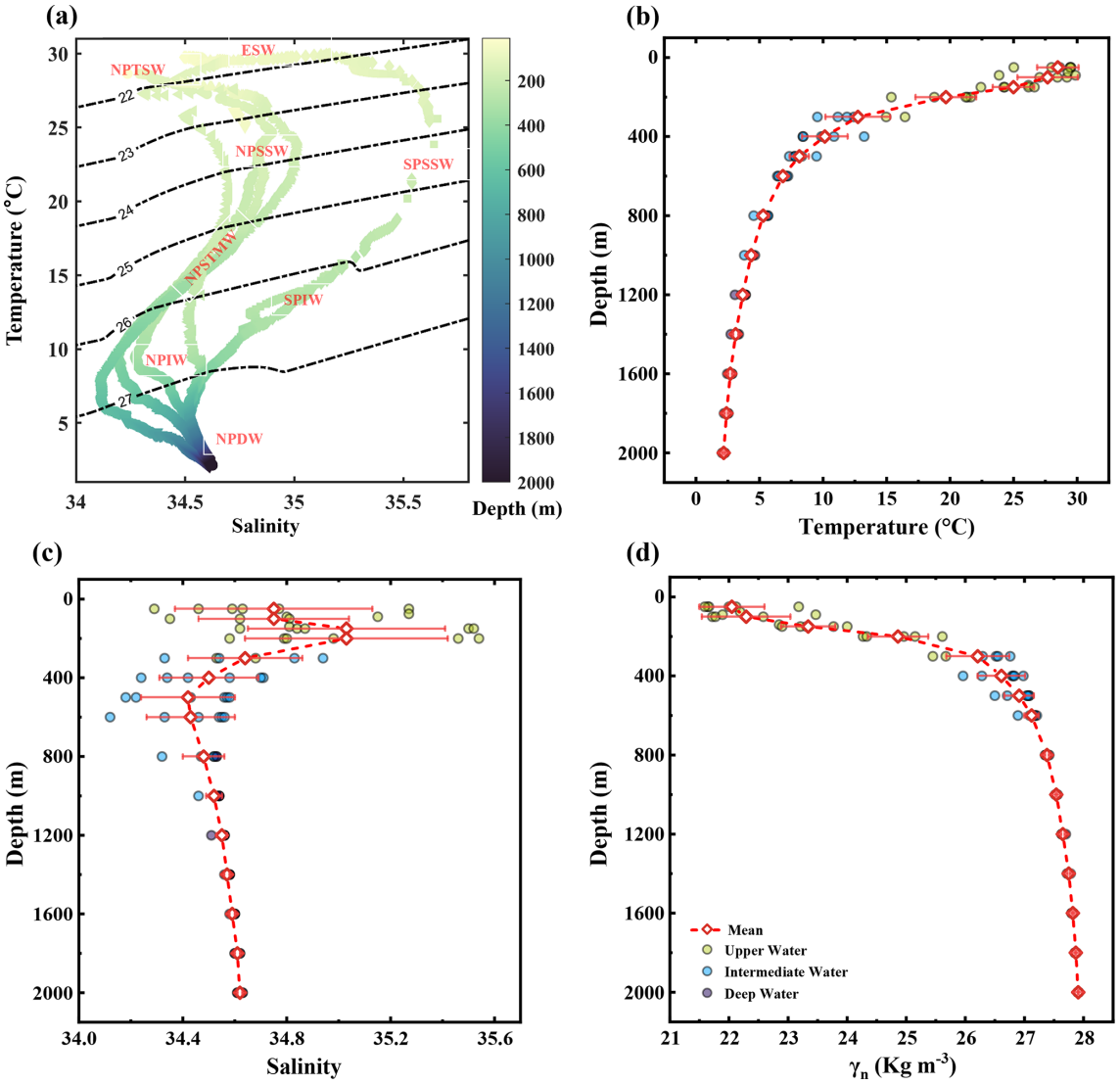

Figure 2. Hydrographic characteristics of the water column. **(a)** Temperature-salinity diagram of six stations, and the vertical profiles of **(b)** temperature, **(c)** salinity, **(d)** neutral density (γ_n). Red diamonds connected by dashed lines and their horizontal error bars denote the mean ± standard deviation of all samples collected at each nominal sampling depth.

in deeper waters. These concentrations were within the low range reported for open ocean environments (Table S1 in the Supplement). After conversion to carbon equivalents using a factor of 0.51 (Engel and Passow, 2001), the TEP-C / POC ratio ranged from 15.45 % to 71.75 %, with a mean of 43.81 ± 14.62 %. The mean ratio was commonly higher than those observed in eutrophic oceanic regions (Table S1). POC concentrations decrease rapidly in the intermediate and deep waters, while the AOU continuously increased (Fig. 3f, g). In contrast, TEP concentrations decrease more slowly and remain within a measurable range even in the deep waters (Fig. 3i).

3.3 Microbial community structure

Among the five identified dominant genera, Pelagibacter, an oligotrophic bacterial genus, and Alteromonas, an opportunistic heterotrophic bacterial genus, had the highest relative abundances, but displayed different vertical patterns (Fig. 4). In the upper waters, Pelagibacter was the most abundant highlighted genus, accounting for 18.4 % of the community. Alteromonas represented a comparable proportion of 16.6 %. Nitrosopumilus, a chemoautotrophic ammonia-oxidizing archaeal genus, accounted for 4.6 %, whereas Halomonas and Alcanivorax were minor components, accounting for 1.3 % and 1.2 %, respectively. The intermediate waters showed a different community composition, the relative abundance of Pelagibacter decreased to 5.0 %, whereas that of Al-

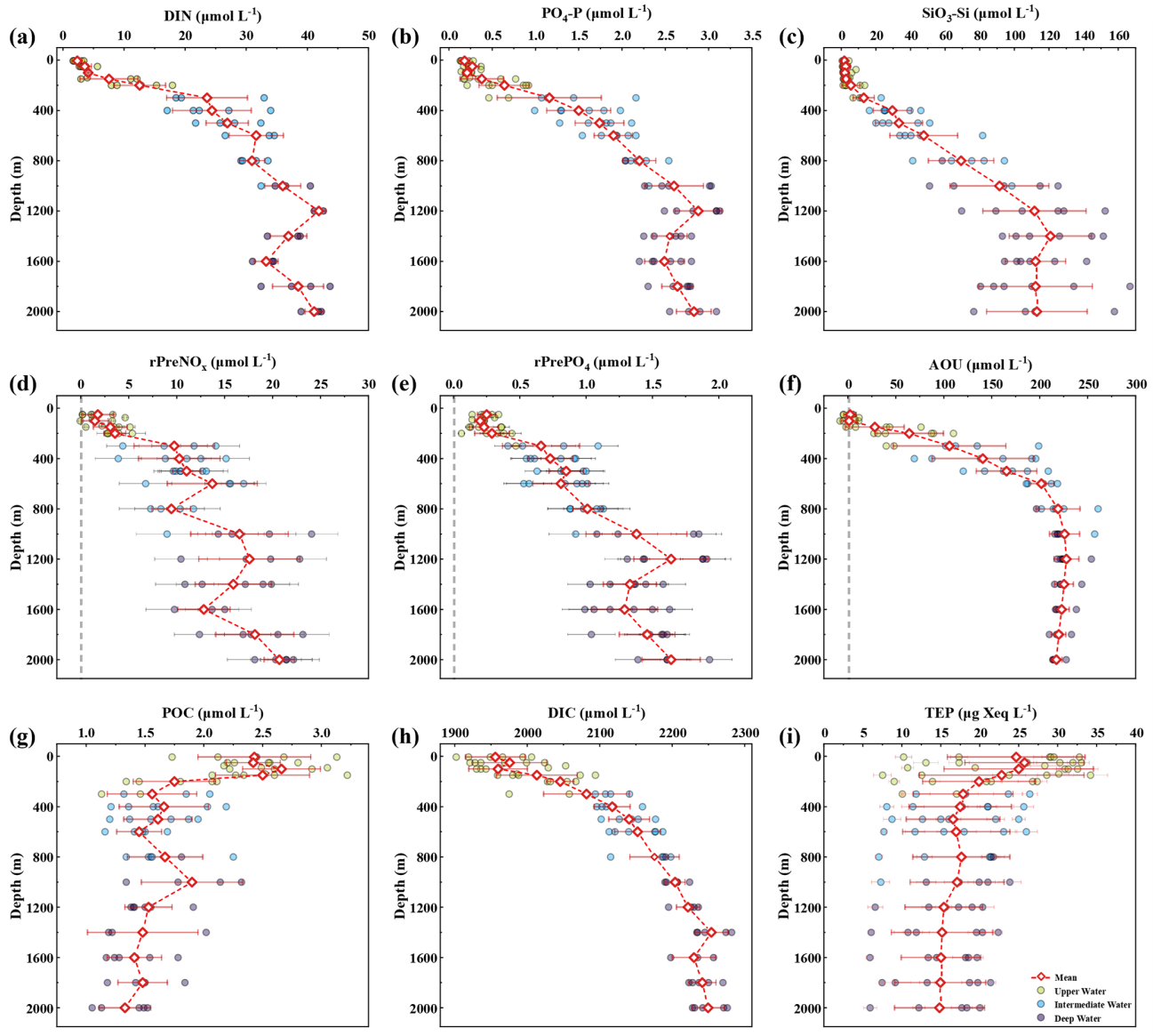

Figure 3. Vertical distributions of chemical and particulate parameters in the water column. Profiles show **(a)** dissolved inorganic nitrogen (DIN), **(b)** phosphate (PO_4-P, as dissolved inorganic phosphorus, DIP), **(c)** silicate (SiO_3-Si, as dissolved inorganic silicon, DSi), **(d)** residual preformed NO_x ($rPreNO_x$), **(e)** residual preformed phosphate ($rPrePO_4$), **(f)** apparent oxygen utilization (AOU), **(g)** particulate organic carbon (POC), **(h)** dissolved inorganic carbon (DIC), **(i)** transparent exopolymer particle (TEP). For $rPreNO_x$ and $rPrePO_4$, each point and its horizontal error bar represent the mean ± standard deviation derived from the 9 parameter combinations for an individual sample. For TEP, each point and its horizontal error bar represent the mean ± standard deviation of triplicate measurements. Red diamonds connected by dashed lines and their horizontal error bars denote the mean ± standard deviation of all samples collected at each nominal sampling depth.

teromonas remained relatively high at 16.2 %. The relative abundance of Nitrosopumilus increased to 6.8 %, and those of Halomonas and Alcanivorax increased to 4.2 % and 3.3 %, respectively. In the deep waters, Alteromonas increased to 22.9 % and became the most abundant identified genus, whereas Pelagibacter declined further to 3.0 %. Halomonas reached its highest relative abundance of 6.3 %, while Nitrosopumilus and Alcanivorax accounted for 5.0 % and 2.5 %, respectively.

4 Discussion

4.1 Spatial variation and controlling factors of nutrient dynamics in TNWP water column

The AOU of the ocean water column is an important indicator of the intensity of organic matter remineralization and oxygen consumption (Sulpis et al., 2023). In the upper waters of the study area, AOU is slightly negative and

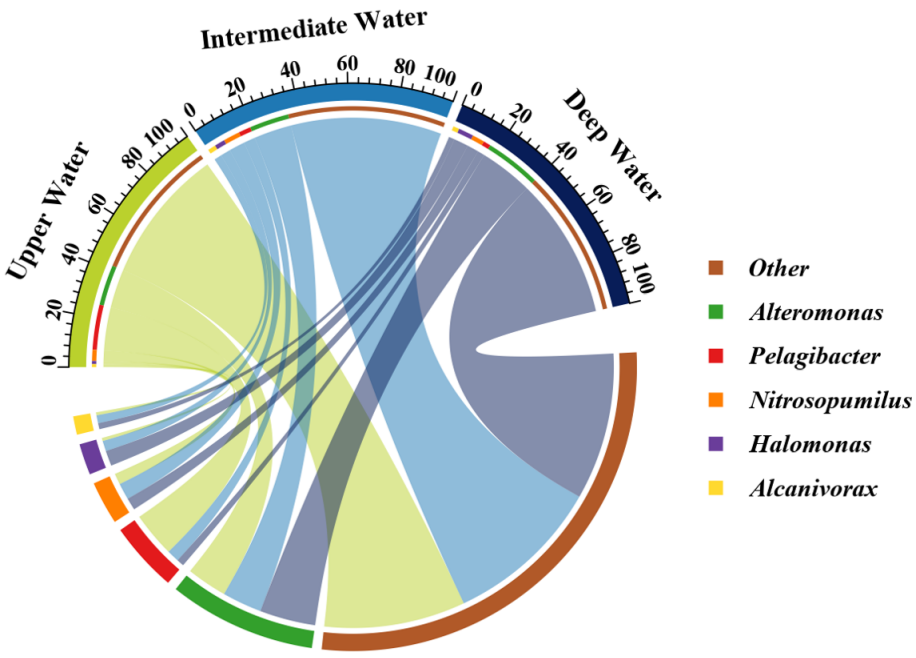

Figure 4. Relative abundance (%) of major microbial genera across the upper, intermediate, and deep waters.

close to zero, reflecting photosynthetic oxygen production and bubble injection. From the upper to the intermediate waters, AOU increases rapidly, indicating intensified organic-matter remineralization dominated by heterotrophic respiration (Fig. 3f). In deep waters, AOU increases to a maximum of $227.80 \pm 8.69\ \mu mol\ L^{-1}$ and then remains relatively stable, suggesting a dynamic balance between oxygen consumption and supply (Fig. 3f). In this study area, the AOU / DIN and AOU / DIP of the entire water column are 6.28 and 86.79, respectively, much lower than the ideal Redfield model (i.e., AOU / DIN = 8.6, AOU / DIP = 138) (Redfield, 1960) and also lower than the reported values from the Atlantic and Indian Oceans (AOU / DIN = 10.6, AOU / DIP = 170) (Anderson and Sarmiento, 1994). Although previous studies have shown that in strongly mixed ocean areas, enhanced water aeration can systematically suppress linear regression slopes (AOU / DIN = 3.1, AOU / DIP = 57.6) (Zhu et al., 2025), our study area is located in the WPWP, where strong stratification inhibits vertical mixing and exchange (Hu et al., 2015). Hence, physical "noise" is weak, and the low ratios observed here are more likely to originate from biogeochemical processes operating within the waters.

To examine how these biogeochemical processes vary across water column, we calculated AOU / nutrient regression slopes separately for the upper, intermediate, and deep waters (Fig. 5). The AOU / DIN value is lowest in the upper waters (6.87), increases in the intermediate waters (7.22), and becomes statistically insignificant in the deep waters ($p > 0.05$) (Fig. 5a). The AOU / DIP slope is higher in the upper waters (116.04), decreasing in the intermediate waters (103.17), and non-significant in the deep waters (Fig. 5b). The low AOU / DIN and AOU / DIP slopes in the upper and intermediate waters indicate greater nutrient accumulation per unit increase in AOU than expected from the classical reference ratios. Limited vertical nutrient supply maintains persistently oligotrophic conditions in the upper water column (Chl *a* in the deep chlorophyll maximum: $0.19–0.31\ \mu g\ L^{-1}$). Under nutrient limitation, phytoplankton may allocate a relatively large proportion of photosynthetically fixed carbon to extracellular polysaccharides and TEP with high C : N ratios rather than to nutrient-rich cellular biomass (Smyth and Letscher, 2023; Curran et al., 2025). The observed TEP-C / POC ratios in the upper waters (mean of $43.81 \pm 14.62\ \%$) indicate that estimated TEP-associated carbon constituted a substantial component of the local POC pool (Fig. 3i, Table S1). Positive ensemble average $rPreNO_x$ and $rPrePO_4$ residuals occurred together with elevated TEP concentrations in the upper water column (Fig. 3d, e, and i). This indicates that measured nutrient concentrations were higher than predicted from AOU under the prescribed DOM and POM remineralization parameters, resulting in a lower AOU / nutrient ratio in the upper waters. Although standing TEP concentrations do not directly quantify production, the substantial contribution of TEP-associated carbon to the local POC pool and its co-occurrence with low AOU / nutrient ratios support carbon allocation to TEP as one plausible contributor to the observed deviations. Future studies should examine whether similarly low AOU / nutrient ratios occur in other ocean regions with comparably high TEP-C / POC ratios to assess the spatial generality of this association. Furthermore, evidence indicates that heterotrophic microorganisms preferentially consume components with low C : N, such as proteins,

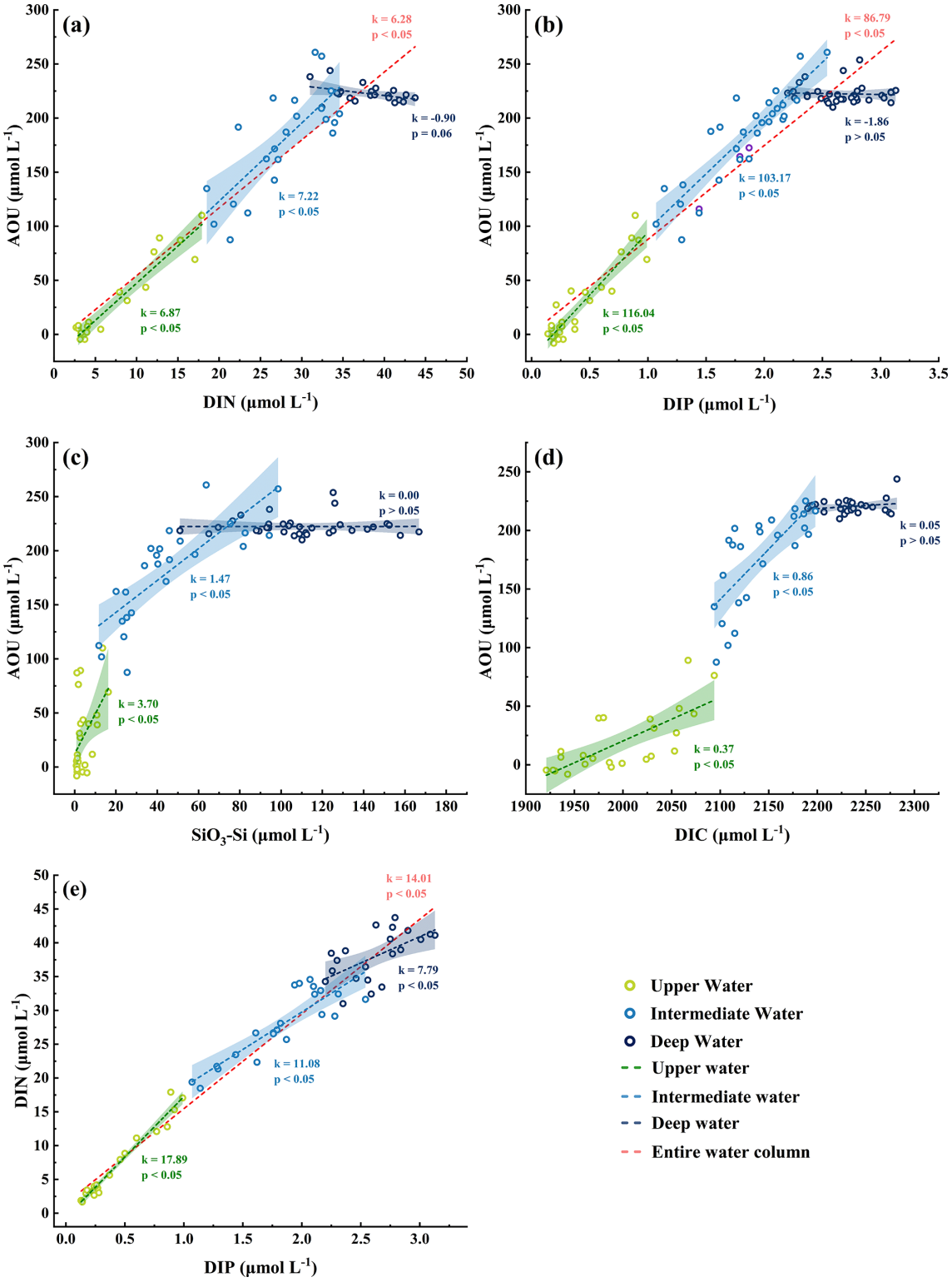

Figure 5. The correlation between apparent oxygen utilization (AOU) and **(a)** dissolved inorganic nitrogen (DIN), **(b)** dissolved inorganic phosphorus (DIP), **(c)** silicate (SiO_3-Si, as dissolved inorganic silicon, DSi), **(d)** dissolved inorganic carbon (DIC), and **(e)** relationship between DIN and DIP. The shaded areas represent the 95 % confidence intervals of the fitted regression lines.

in organic matter during aerobic respiration (Hwang et al., 2006; Tian et al., 2025). Therefore, in the intermediate waters, preferential degradation of relatively nutrient rich and labile organic components may enhance nutrient regeneration relative to bulk organic carbon oxidation, thereby contributing to the low AOU / nutrient slopes (Fig. 5a, b). In the deep waters, the absence of significant AOU / nutrients relationships precludes the calculation of meaningful remineralization ratios. In this depth horizon, AOU remains relatively stable whereas nutrient concentrations continue to increase, suggesting that their distributions are governed primarily by the cumulative effects of water-mass aging, lateral transport, and diverse biogeochemical transformations operating on different timescales. Among these, nitrification mediated by ammonia-oxidizing archaea such as *Nitrosopumilus* may consume oxygen without concomitant phosphorus regeneration (Martens-Habbena et al., 2009), while DOP hydrolysis associated with *Alteromonas* may mobilize phosphate independently of bulk organic matter oxidation (Saavedra et al., 2025). Collectively, these processes likely contribute to the observed decoupling between AOU and nutrients in the deep ocean.

Unlike DIN and DIP, SiO_3-Si and AOU do not exhibit a clear linear relationship in the entire water column, but instead show distinct vertical stratification. In the upper waters, intense silicate uptake by phytoplankton such as diatoms drives concentrations to near-zero values (Fig. 5c) (Brzezinski et al., 2024). In the intermediate waters, the variation in silicate concentration is mainly influenced by diatom deposition and remineralization. As AOU increases, silicates are rapidly released, resulting in an AOU / SiO_3-Si ratio (1.47) lower in these waters than in the upper waters (3.70) (Fig. 5c). In the deep waters, AOU tends to remain nearly constant, whereas SiO_3-Si concentration continued to increase owing to the delayed dissolution of siliceous biogenic debris (Yu et al., 2022). It is estimated that about two-thirds of biogenic silica dissolves at depths shallower than 2000 m, with the remainder released more slowly at greater depths (Tréguer and De La Rocha, 2013). Consequently, SiO_3-Si levels at depth are largely decoupled from organic matter supply and exhibit no significant linear relationship with AOU (Fig. 5c). A similar decoupling between biological consumption and accumulation is observed in the distribution of DIC, which exhibits a characteristic three-stage pattern from upper to deep waters (Fig. 5d). In upper waters, photosynthesis consumes DIC; however, this signal is masked by intense air-sea CO_2 exchange, which leads to a net increase in DIC and consequently a low AOU / DIC ratio of 0.37 (Ito and Reinhard, 2025). In intermediate waters, organic matter decomposition dominates, and DIC increases rapidly with increasing AOU (AOU / DIC = 0.86, Fig. 5d) (Hu et al., 2016). In deep waters, AOU remains stable while DIC accelerates again, due to the accumulation of respired CO_2 from above and enhanced calcium carbonate dissolution with depth (Chen et al., 2022; Feely et al., 2004).

Furthermore, DIN and DIP in each layers of the study area show a strong linear correlation, and the slope decreases progressively from 17.89 in the upper waters to 11.08 in the intermediate waters and further to 7.79 in the deep waters, with an overall slope of 14.01, which is lower than the Redfield ratio (Fig. 5e). The overall low N : P ratio (14.01) and its vertical decline reflect that phosphorus is regenerated more efficiently than nitrogen in this region. Denitrification, which removes fixed nitrogen, can lower the N : P ratio. However, classical water-column denitrification typically requires dissolved oxygen concentrations below 5 $\mu mol\,L^{-1}$ (Deutsch et al., 2011). In the present study, the minimum observed oxygen concentration exceeds 55 $\mu mol\,L^{-1}$, making extensive pelagic denitrification unlikely. Denitrification may nevertheless occur within particles suspended in oxygenated water when respiratory oxygen demand exceeds oxygen supply, particularly in large particles with high respiratory activity (Ploug, 2001; Ploug et al., 2008). The importance of this process depends on particle abundance and size distribution (Bianchi et al., 2018), and has been shown to increase with particle size and concentration in oxygenated coastal waters with high particle loads (Wan et al., 2023). In our study, POC and TEP concentrations were within the lower reported ranges (Table S1), indicating relatively low particle loads. Although these bulk measurements cannot exclude denitrification within individual particles, they suggest that this process was unlikely to dominate the observed DIN : DIP pattern. Alternatively, enhanced phosphate release from dissolved organic phosphorus (DOP) via alkaline phosphatase (APase) activity represents one potential mechanism. Although direct APase measurements were not made in this study, previous work has demonstrated that APase produced by Alteromonas can maintain high expression and abundance under phosphorus-limited conditions and even in deeper waters where inorganic phosphorus is not scarce (Saavedra et al., 2025). Given that Alteromonas accounts for a high proportion in all waters (Fig. 4), it is plausible that this genus contributes to DOP hydrolysis and thereby to the observed low N : P ratio.

4.2 Microbial regulation of non-Redfield stoichiometry in organic matter degradation

The low AOU / DIN (6.28) and AOU / DIP (86.79) ratios observed in the TNWP result from the metabolic strategies of the resident microbial community. Within the study area, *Pelagibacter* and *Alteromonas* emerge as the two most abundant bacterial genera, their complementary metabolic capabilities directly modulate the coupling between organic carbon oxidation and nutrient regeneration, thereby driving the observed deviations from Redfield stoichiometry. *Pelagibacter* exhibits a significant positive correlation with organic matter and a negative correlation with inorganic nutrients (Fig. 6), consistent with its streamlined genome and oligotrophic adaptive strategy (Giovannoni, 2017; Carini et al.,

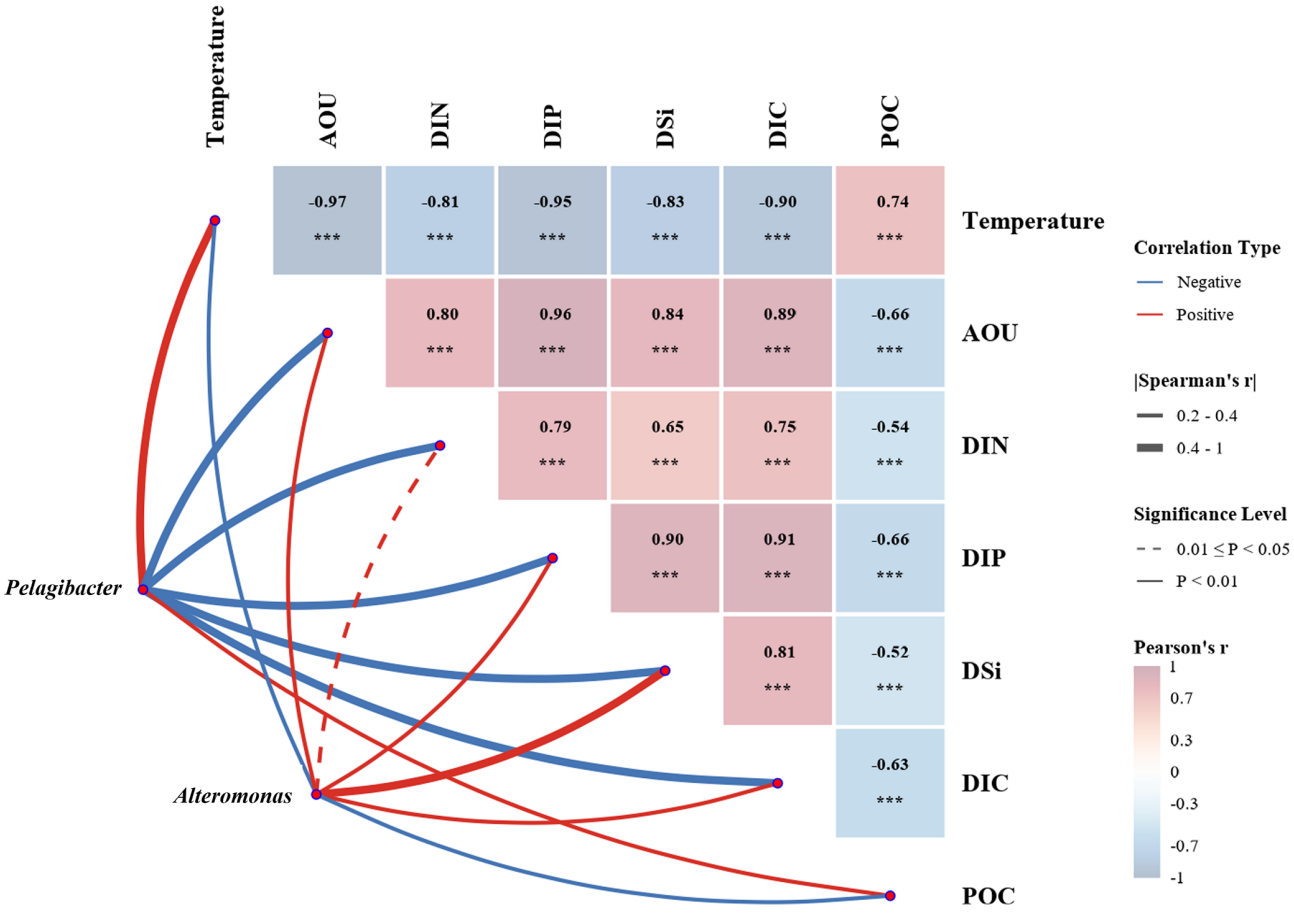

Figure 6. Correlation between dominant microbes and environmental variables. Heatmaps were based on Pearson correlation analysis among environmental variables in the study area (*** represents $p < 0.01$), and Spearman correlation analysis between *Pelagibacter* / *Alteromonas* and environmental variables.

2013). This bacterium lacks the ability to synthesize several essential metabolites and relies on exogenous supply, but its cell surface is enriched with high-affinity transport proteins that enable efficient uptake of small-molecule dissolved organic matter (Giovannoni, 2017). Critically, *Pelagibacter* selectively removes nitrogen-rich organic substrates such as amino acids and proteins, while leaving behind carbon-rich polymers (Malmstrom et al., 2005).

In contrast, *Alteromonas* displays the opposite environmental correlation pattern: showing a significantly positive correlation with inorganic nutrients and a negative correlation with POC (Fig. 6), reflecting its role as a particle-associated opportunist with a versatile genome encoding diverse polysaccharide-degrading enzymes (Koch et al., 2019; Lopez-Perez et al., 2012). This genus is a major contributor to alkaline phosphatase gene expression (particularly phoD and phoX) and enzymatic activity (Saavedra et al., 2025). Under phosphorus-limited conditions, these enzymes hydrolyze dissolved organic phosphorus (DOP) to release bioavailable phosphate (Saavedra et al., 2025). *Alteromonas* was abundant in all waters (Fig. 4), resulting in faster phosphorus regeneration than nitrogen regeneration in the study area, leading to an observed DIN : DIP ratio of approximately 14 : 1, lower than the Redfield value of 16 : 1 (Fig. 5e). Beyond these two dominant genera, the ammonia-oxidizing archaeon *Nitrosopumilus*, which is abundant in the intermediate waters (Fig. 4), can mediate high-affinity nitrification and consume oxygen even at extremely low ammonium concentrations ($< 10\,\mathrm{nmol\,L^{-1}}$) (Martens-Habbena et al., 2009).

The ecological division of labor between these functional groups creates a vertically structured processing network: *Pelagibacter* sustains the microbial loop and small-molecule cycling in oligotrophic upper waters through high-affinity uptake, while *Alteromonas* dominates the degradation of settling TEP and other complex polymers, releasing inorganic nutrients in deeper waters (Robertson et al., 2024). This functional differentiation enables the preferential degradation of low C : N substrates, coupled with active phosphorus scavenging from organic pools, driving the system toward enhanced nutrient regeneration relative to organic carbon oxidation, thereby maintaining a dynamic equilibrium in its biogeochemical cycles and overall ecosystem function.

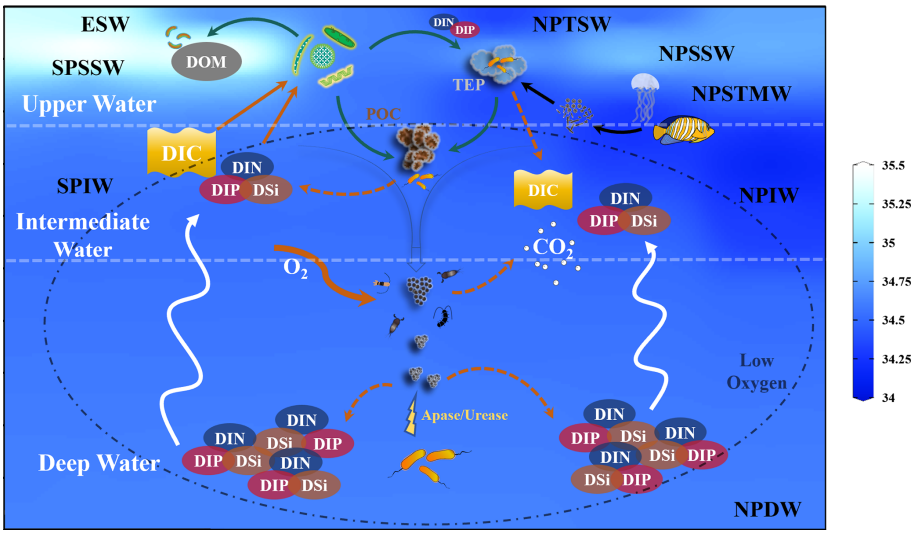

Figure 7. Schematic diagram of coupled physical-biogeochemical-microbial controls on carbon and nutrient cycling in the study area with a salinity background.

4.3 Coupled physical-biogeochemical-microbial controls on carbon and nutrient cycling in the TNWP

The strong vertical stratification of the TNWP creates a multi-water-mass structure. Nutrients are primarily retained in deep reservoirs and remain chronically depleted in upper waters. Nutrient regeneration in intermediate waters relies mainly on the release during organic matter degradation (Hirose and Kamiya, 2003). In this nutrient-poor environment, the synthesis of TEP with a high C : N ratio creates an imbalance between oxygen production and nitrate consumption (Fig. 3i), leading to positive anomalies in the $rPrePO_4$ and $rPreNO_x$ in surface waters (Fig. 3d, e) (Curran et al., 2025). POM is gradually degraded during settling, while intermediate and deep waters are active areas for heterotrophic respiration. It is estimated that approximately 90 % of the organic matter exported to this area is remineralized and releases CO_2 (Robinson et al., 2010). This process consumes a large amount of DO, and the strong stratification hinders the timely replenishment of DO in the intermediate and deep waters, thereby forming low oxygen zones in these waters (Fig. 7).

Simultaneously, nutrient release also mainly occurs in the intermediate and deep waters, exhibiting a clear regeneration gradient from shallow to deep (Fig. 3a–c) (Hirose and Kamiya, 2003). The distribution patterns and functional traits of key bacteria in the water column are closely linked to their distinct ecological niches. *Pelagibacter* is abundant in oligotrophic upper waters (Fig. 4), and its streamlined genome and metabolic mechanisms enable it to drive the remineralization of small-molecule organic carbon and nutrient recycling through slow but continuous growth (Sun et al., 2011). *Alteromonas* relies on a diverse enzyme system to efficiently respond to organic substrates, thereby utilizing complex polymers (Koch et al., 2019). This functional differentiation within the microbial community maintains the slow cycling of dissolved organic matter under oligotrophic conditions and ensures the efficient degradation of complex polymeric organic matter when available, thereby regulating both the pathways and the intensity of carbon, nitrogen, and phosphorus cycling in the water column.

5 Conclusions

The oligotrophic tropical Northwest Pacific is characterized by pronounced vertical stratification, which retains nutrients at depth and sustains chronic nutrient limitation in the upper ocean. In surface waters, phytoplankton respond to nutrient stress by producing carbon rich transparent exopolymer particles, altering the balance among carbon fixation, oxygen production, and nutrient assimilation. In intermediate waters, selective transformation of labile and nutrient rich components promotes nitrogen and phosphorus regeneration while carbon rich polysaccharides persist longer. These depth dependent changes are accompanied by shifts in microbial function, with *Pelagibacter* contributing to the recycling of small organic molecules in upper waters and *Alteromonas* participating in polymer degradation and potentially in phosphorus regeneration through alkaline phosphatase activity at greater depths. In deep water, the absence of significant AOU to nutrient relationships indicates that nutrient accumulation is increasingly influenced by the aging of waters, additional microbial and geochemical processes. The low integrated AOU / DIN and AOU / DIP slopes of 6.28 and 86.79 therefore reflect the combined effects of distinct processes operating among waters. These findings show that vertical changes

in organic matter production, export, and microbial transformation can substantially modify nutrient regeneration stoichiometry and should be considered when representing carbon and nutrient cycling in oligotrophic ocean models.

Data availability. The data used in this paper are available at Figshare (https://doi.org/10.6084/m9.figshare.31841125; Tian, 2026).

Supplement. The supplement related to this article is available online at https://doi.org/10.5194/bg-23-6431-2026-supplement.

Author contributions. DT carried out the investigation, developed the methodology, performed data curation and visualization, and prepared the original draft. XL and YX acquired the funding, and reviewed and edited the manuscript. FZ provided resources. JM, SL, and MIUK reviewed and edited the manuscript. WW conceptualized the study, and reviewed and edited the manuscript.

Competing interests. The contact author has declared that none of the authors has any competing interests.

Disclaimer. Publisher's note: Copernicus Publications remains neutral with regard to jurisdictional claims made in the text, published maps, institutional affiliations, or any other geographical representation in this paper. The authors bear the ultimate responsibility for providing appropriate place names. Views expressed in the text are those of the authors and do not necessarily reflect the views of the publisher.

Acknowledgements. We thank the crews of the R/V *Kexue* for sampling assistance during the NORC2021-09 cruise, and the two anonymous reviewers for their constructive comments that improved this manuscript.

Financial support. This research has been supported by the National Natural Science Foundation of China (grant nos. 42530401 and 42476204).

Review statement. This paper was edited by Hermann Bange and reviewed by two anonymous referees.

References

Álvarez-Salgado, X. A., Álvarez, M., Brea, S., Mèmery, L., and Messias, M. J.: Mineralization of biogenic materials in the water masses of the South Atlantic Ocean. II: Stoichiometric ratios and mineralization rates, Prog. Oceanogr., 123, 24–37, https://doi.org/10.1016/j.pocean.2013.12.009, 2014.

Anderson, L. A. and Sarmiento, J. L.: Redfield ratios of remineralization determined by nutrient data analysis, Global Biogeochem. Cy., 8, 65–80, https://doi.org/10.1029/93gb03318, 1994.

Bianchi, D., Weber, T. S., Kiko, R., and Deutsch, C.: Global niche of marine anaerobic metabolisms expanded by particle microenvironments, Nat. Geosci., 11, 263–268, https://doi.org/10.1038/s41561-018-0081-0, 2018.

Bittar, T. B., Passow, U., Hamaraty, L., Bidle, K. D., and Harvey, E. L.: An updated method for the calibration of transparent exopolymer particle measurements, Limnol. Oceanogr. Methods., 16, 621–628, https://doi.org/10.1002/lom3.10268, 2018.

Bryan, J. R., Rlley, J. P., and Williams, P. J. L.: A winkler procedure for making precise measurements of oxygen concentration for productivity and related studies, J. Exp. Mar. Biol. Ecol., 21, 191–197, https://doi.org/10.1016/0022-0981(76)90114-3, 1976.

Brzezinski, M. A., Johnson, L., Estapa, M., Clevenger, S., Roca-Martí, M., Romanelli, E., Buck, K. N., Jenkins, B. D., and Jones, J. L.: Physical Mechanisms Sustaining Silica Production Following the Demise of the Diatom Phase of the North Atlantic Spring Phytoplankton Bloom During EXPORTS, Global Biogeochem. Cy., 38, e2023GB008048, https://doi.org/10.1029/2023gb008048, 2024.

Calleja, M. L., Al-Otaibi, N., and Moran, X. A. G.: Dissolved organic carbon contribution to oxygen respiration in the central Red Sea, Sci. Rep., 9, 4690, https://doi.org/10.1038/s41598-019-40753-w, 2019.

Carini, P., Steindler, L., Beszteri, S., and Giovannoni, S. J.: Nutrient requirements for growth of the extreme oligotroph 'Candidatus Pelagibacter ubique' HTCC1062 on a defined medium, ISME J., 7, 592–602, https://doi.org/10.1038/ismej.2012.122, 2013.

Chen, H., Haumann, F. A., Talley, L. D., Johnson, K. S., and Sarmiento, J. L.: The Deep Ocean's Carbon Exhaust, Global Biogeochem. Cy., 36, e2021GB007156, https://doi.org/10.1029/2021GB007156, 2022.

Curran, K., Villareal, T. A., and Letscher, R. T.: A time series analysis of transparent exopolymer particle distributions and C : N stoichiometry in the subtropical North Pacific: a key process in net community production and preformed nitrate anomalies?, Biogeosciences, 22, 3515–3531, https://doi.org/10.5194/bg-22-3515-2025, 2025.

Dai, M., Luo, Y. W., Achterberg, E. P., Browning, T. J., Cai, Y., Cao, Z., Chai, F., Chen, B., Church, M. J., Ci, D., Du, C., Gao, K., Guo, X., Hu, Z., Kao, S. J., Laws, E. A., Lee, Z., Lin, H., Liu, Q., Liu, X., Luo, W., Meng, F., Shang, S., Shi, D., Saito, H., Song, L., Wan, X. S., Wang, Y., Wang, W. L., Wen, Z., Xiu, P., Zhang, J., Zhang, R., and Zhou, K.: Upper Ocean Biogeochemistry of the Oligotrophic North Pacific Subtropical Gyre: From Nutrient Sources to Carbon Export, Rev. Geophys., 61, e2022RG000800, https://doi.org/10.1029/2022rg000800, 2023.

Delaigue, L., Sulpis, O., Reichart, G. J., and Humphreys, M. P.: The Changing Biological Carbon Pump of the South Atlantic Ocean, Global Biogeochem. Cy., 38, e2024GB008202, https://doi.org/10.1029/2024gb008202, 2024.

Deutsch, C., Brix, H., Ito, T., Frenzel, H., and Thompson, L.: Climate-forced variability of ocean hypoxia, Science, 333, 336–339, https://doi.org/10.1126/science.1202422, 2011.

Digernes, M. G., Bodur, Y. V., Amargant-Arumí, M., Müller, O., Hawkes, J. A., Kohler, S. G., Dietrich, U., Reigstad, M., and Paulsen, M. L.: Contrasting seasonal patterns in particle aggregation and dissolved organic matter transformation in a sub-Arctic fjord, Biogeosciences, 22, 601–623, https://doi.org/10.5194/bg-22-601-2025, 2025.

Engel, A. and Passow, U.: Carbon and nitrogen content of transparent exopolymer particles (TEP) in relation to their Alcian Blue adsorption, Mar. Ecol. Prog. Ser., 219, 1–10, https://doi.org/10.3354/meps219001, 2001.

Feely, R. A., Sabine, C. L., Lee, K., Berelson, W., Kleypas, J., Fabry, V. J., and Millero, F. J.: Impact of anthropogenic CO_2 on the $CaCO_3$ system in the oceans, Science, 305, 362–366, https://doi.org/10.1126/science.1097329, 2004.

Friedlingstein, P., O'Sullivan, M., Jones, M. W., Andrew, R. M., Hauck, J., Landschützer, P., Le Quéré, C., Li, H., Luijkx, I. T., Olsen, A., Peters, G. P., Peters, W., Pongratz, J., Schwingshackl, C., Sitch, S., Canadell, J. G., Ciais, P., Jackson, R. B., Alin, S. R., Arneth, A., Arora, V., Bates, N. R., Becker, M., Bellouin, N., Berghoff, C. F., Bittig, H. C., Bopp, L., Cadule, P., Campbell, K., Chamberlain, M. A., Chandra, N., Chevallier, F., Chini, L. P., Colligan, T., Decayeux, J., Djeutchouang, L. M., Dou, X., Duran Rojas, C., Enyo, K., Evans, W., Fay, A. R., Feely, R. A., Ford, D. J., Foster, A., Gasser, T., Gehlen, M., Gkritzalis, T., Grassi, G., Gregor, L., Gruber, N., Gürses, Ö., Harris, I., Hefner, M., Heinke, J., Hurtt, G. C., Iida, Y., Ilyina, T., Jacobson, A. R., Jain, A. K., Jarníková, T., Jersild, A., Jiang, F., Jin, Z., Kato, E., Keeling, R. F., Klein Goldewijk, K., Knauer, J., Korsbakken, J. I., Lan, X., Lauvset, S. K., Lefèvre, N., Liu, Z., Liu, J., Ma, L., Maksyutov, S., Marland, G., Mayot, N., McGuire, P. C., Metzl, N., Monacci, N. M., Morgan, E. J., Nakaoka, S.-I., Neill, C., Niwa, Y., Nützel, T., Olivier, L., Ono, T., Palmer, P. I., Pierrot, D., Qin, Z., Resplandy, L., Roobaert, A., Rosan, T. M., Rödenbeck, C., Schwinger, J., Smallman, T. L., Smith, S. M., Sospedra-Alfonso, R., Steinhoff, T., Sun, Q., Sutton, A. J., Séférian, R., Takao, S., Tatebe, H., Tian, H., Tilbrook, B., Torres, O., Tourigny, E., Tsujino, H., Tubiello, F., van der Werf, G., Wanninkhof, R., Wang, X., Yang, D., Yang, X., Yu, Z., Yuan, W., Yue, X., Zaehle, S., Zeng, N., and Zeng, J.: Global Carbon Budget 2024, Earth Syst. Sci. Data, 17, 965–1039, https://doi.org/10.5194/essd-17-965-2025, 2025.

Giovannoni, S. J.: SAR11 Bacteria: The Most Abundant Plankton in the Oceans, Ann. Rev. Mar. Sci., 9, 231–255, https://doi.org/10.1146/annurev-marine-010814-015934, 2017.

Guo, J., Zhou, B., Achterberg, E. P., Yuan, H., Song, J., Duan, L., and Li, X.: Rapid Cycling of Bacterial Particulate Organic Matter in the Upper Layer of the Western Pacific Warm Pool, Geophys. Res. Lett., 50, e2023GL102896, https://doi.org/10.1029/2023gl102896, 2023.

Hirose, K. and Kamiya, H.: Vertical Nutrient Distributions in the Western North Pacific Ocean: Simple Model for Estimating Nutrient Upwelling, Export Flux and Consumption Rates, J. Oceanogr., 59, 149–161, https://doi.org/10.1023/a:1025535003841, 2003.

Hu, D., Wu, L., Cai, W., Gupta, A. S., Ganachaud, A., Qiu, B., Gordon, A. L., Lin, X., Chen, Z., Hu, S., Wang, G., Wang, Q., Sprintall, J., Qu, T., Kashino, Y., Wang, F., and Kessler, W. S.: Pacific western boundary currents and their roles in climate, Nature, 522, 299–308, https://doi.org/10.1038/nature14504, 2015.

Hu, X., Cai, W.-J., Rabalais, N. N., and Xue, J.: Coupled oxygen and dissolved inorganic carbon dynamics in coastal ocean and its use as a potential indicator for detecting water column oil degradation, Deep-Sea Res. Pt. II, 129, 311–318, https://doi.org/10.1016/j.dsr2.2014.01.010, 2016.

Hwang, J., Druffel, E. R. M., Eglinton, T. I., and Repeta, D. J.: Source(s) and cycling of the nonhydrolyzable organic fraction of oceanic particles, Geochim. Cosmochim. Ac., 70, 5162–5168, https://doi.org/10.1016/j.gca.2006.07.020, 2006.

Ito, T. and Reinhard, C. T.: A New Framework for the Attribution of Air-Sea CO_2 Exchange, Global Biogeochem. Cy., 39, e2024GB008346, https://doi.org/10.1029/2024gb008346, 2025.

Ito, T., Follows, M. J., and Boyle, E. A.: Is AOU a good measure of respiration in the oceans?, Geophys. Res. Lett., 31, L17305, https://doi.org/10.1029/2004gl020900, 2004.

Jian, Z., Wang, Y., Dang, H., Mohtadi, M., Rosenthal, Y., Lea, D. W., Liu, Z., Jin, H., Ye, L., Kuhnt, W., and Wang, X.: Warm pool ocean heat content regulates ocean-continent moisture transport, Nature, 612, 92–99, https://doi.org/10.1038/s41586-022-05302-y, 2022.

Kharbush, J. J., Close, H. G., Van Mooy, B. A. S., Arnosti, C., Smittenberg, R. H., Le Moigne, F. A. C., Mollenhauer, G., Scholz-Böttcher, B., Obreht, I., Koch, B. P., Becker, K. W., Iversen, M. H., and Mohr, W.: Particulate Organic Carbon Deconstructed: Molecular and Chemical Composition of Particulate Organic Carbon in the Ocean, Front. Mar. Sci., 7, 518, https://doi.org/10.3389/fmars.2020.00518, 2020.

Koch, H., Freese, H. M., Hahnke, R. L., Simon, M., and Wietz, M.: Adaptations of Alteromonas sp. 76-1 to Polysaccharide Degradation: A CAZyme Plasmid for Ulvan Degradation and Two Alginolytic Systems, Front. Microbiol., 10, 504, https://doi.org/10.3389/fmicb.2019.00504, 2019.

Kodama, T., Kurogi, H., Okazaki, M., Jinbo, T., Chow, S., Tomoda, T., Ichikawa, T., and Watanabe, T.: Vertical distribution of transparent exopolymer particle (TEP) concentration in the oligotrophic western tropical North Pacific, Mar. Ecol. Prog. Ser., 513, 29–37, https://doi.org/10.3354/meps10954, 2014.

Körtzinger, A., Hedges, J. I., and Quay, P. D.: Redfield ratios revisited: Removing the biasing effect of anthropogenic CO_2, Limnol. Oceanogr., 46, 964–970, https://doi.org/10.4319/lo.2001.46.4.0964, 2001.

Letscher, R. T. and Villareal, T. A.: Evaluation of the seasonal formation of subsurface negative preformed nitrate anomalies in the subtropical North Pacific and North Atlantic, Biogeosciences, 15, 6461–6480, https://doi.org/10.5194/bg-15-6461-2018, 2018.

Liu, W., Zhao, F., Li, X., Zheng, S., Li, L., Zhao, R., and Xu, K.: Enhanced nutrient supply promotes mutualistic interactions between cyanobacteria and bacteria in oligotrophic ocean, Proc. R. Soc. B. Biol. Sci., 291, 20240788, https://doi.org/10.1098/rspb.2024.0788, 2024.

Longhurst, A. R. and Glen Harrison, W.: The biological pump: Profiles of plankton production and consumption in the upper ocean, Prog. Oceanogr., 22, 47–123, https://doi.org/10.1016/0079-6611(89)90010-4, 1989.

Lopez-Perez, M., Gonzaga, A., Martin-Cuadrado, A. B., Onyshchenko, O., Ghavidel, A., Ghai, R., and Rodriguez-Valera, F.: Genomes of surface isolates of Alteromonas macleodii: the life of a widespread marine opportunistic copiotroph, Sci. Rep., 2, 696, https://doi.org/10.1038/srep00696, 2012.

Ma, J., Song, J., Li, X., Yuan, H., Li, N., Duan, L., and Wang, Q.: Control factors of DIC in the Y3 seamount waters of the Western Pacific Ocean, J. Oceanol. Limnol., 38, 1215–1224, https://doi.org/10.1007/s00343-020-9314-3, 2020.

Ma, J., Song, J., Li, X., Wang, Q., Yuan, H., Li, N., and Duan, L.: Analysis of differences in nutrients chemistry in seamount seawaters in the Kocebu and M4 seamounts in Western Pacific Ocean, J. Oceanol. Limnol., 39, 1662–1674, https://doi.org/10.1007/s00343-020-0239-7, 2021a.

Ma, J., Song, J., Li, X., Wang, Q., Zhong, G., Yuan, H., Li, N., and Duan, L.: The OMZ and Its Influence on POC in the Tropical Western Pacific Ocean: Based on the Survey in March 2018, Front. Earth Sci., 9, 632229, https://doi.org/10.3389/feart.2021.632229, 2021b.

Ma, J., Li, X., Song, J., Wang, Q., Wen, L., Xu, K., Zhong, G., Dai, J., Xing, J., and Tian, D.: Relationship and stratification of multiple marine ecological indicators: A case study in the M2 seamount area of the Western Pacific Ocean, Ecol. Indic., 146, 109804, https://doi.org/10.1016/j.ecolind.2022.109804, 2023.

Malmstrom, R. R., Cottrell, M. T., Elifantz, H., and Kirchman, D. L.: Biomass production and assimilation of dissolved organic matter by SAR11 bacteria in the Northwest Atlantic Ocean, Appl. Environ. Microbiol., 71, 2979–2986, https://doi.org/10.1128/AEM.71.6.2979-2986.2005, 2005.

Martens-Habbena, W., Berube, P. M., Urakawa, H., de la Torre, J. R., and Stahl, D. A.: Ammonia oxidation kinetics determine niche separation of nitrifying Archaea and Bacteria, Nature, 461, 976–979, https://doi.org/10.1038/nature08465, 2009.

Ploug, H.: Small-scale oxygen fluxes and remineralization in sinking aggregates, Limnol. Oceanogr., 46, 1624–1631, https://doi.org/10.4319/lo.2001.46.7.1624, 2001.

Ploug, H., Iversen, M. H., and Fischer, G.: Ballast, sinking velocity, and apparent diffusivity within marine snow and zooplankton fecal pellets: Implications for substrate turnover by attached bacteria, Limnol. Oceanogr., 53, 1878–1886, https://doi.org/10.4319/lo.2008.53.5.1878, 2008.

Radenac, M.-H., Messié, M., Léger, F., and Bosc, C.: A very oligotrophic zone observed from space in the equatorial Pacific warm pool, Remote Sens. Environ., 134, 224–233, https://doi.org/10.1016/j.rse.2013.03.007, 2013.

Redfield, A. C.: The biological control of chemical factors in the environment, Sci. Prog., 11, 150–170, 1960.

Robertson, J. M., Garza, E. A., Stubbusch, A. K. M., Dupont, C. L., Hwa, T., and Held, N. A.: Marine bacteria Alteromonas spp. require UDP-glucose-4-epimerase for aggregation and production of sticky exopolymer, mBio., 15, e0003824, https://doi.org/10.1128/mbio.00038-24, 2024.

Robinson, C., Steinberg, D. K., Anderson, T. R., Arístegui, J., Carlson, C. A., Frost, J. R., Ghiglione, J.-F., Hernández-León, S., Jackson, G. A., Koppelmann, R., Quéguiner, B., Ragueneau, O., Rassoulzadegan, F., Robison, B. H., Tamburini, C., Tanaka, T., Wishner, K. F., and Zhang, J.: Mesopelagic zone ecology and biogeochemistry – a synthesis, Deep-Sea Res. Pt. II, 57, 1504–1518, https://doi.org/10.1016/j.dsr2.2010.02.018, 2010.

Saavedra, D. E. M., Gonzalez, J. M., Klaushofer, K., Breyer, E., Afjehi-Sadat, L., Bulgheresi, S., Liao, L., Dong, X., Patrick, W. M., and Baltar, F.: Multifunctionally diverse alkaline phosphatases of Alteromonas drive the phosphorus cycle in the ocean, Nat. Commun., 16, 9789, https://doi.org/10.1038/s41467-025-64455-2, 2025.

Schlitzer, R.: Ocean Data View, http://odv.awi.de (last access: 11 September 2026), 2026.

Singh, A., Baer, S. E., Riebesell, U., Martiny, A. C., and Lomas, M. W.: C : N : P stoichiometry at the Bermuda Atlantic Time-series Study station in the North Atlantic Ocean, Biogeosciences, 12, 6389–6403, https://doi.org/10.5194/bg-12-6389-2015, 2015.

Smith, C. R., De Leo, F. C., Bernardino, A. F., Sweetman, A. K., and Arbizu, P. M.: Abyssal food limitation, ecosystem structure and climate change, Trends Ecol. Evol., 23, 518–528, https://doi.org/10.1016/j.tree.2008.05.002, 2008.

Smyth, A. J. and Letscher, R. T.: Spatial and temporal occurrence of preformed nitrate anomalies in the subtropical North Pacific and North Atlantic oceans, Mar. Chem., 252, 104248, https://doi.org/10.1016/j.marchem.2023.104248, 2023.

Sulpis, O., Trossman, D. S., Holzer, M., Jeansson, E., Lauvset, S. K., and Middelburg, J. J.: Respiration Patterns in the Dark Ocean, Global Biogeochem. Cy., 37, e2023GB007747, https://doi.org/10.1029/2023gb007747, 2023.

Sun, C., Xu, J., Liu, Z., Tong, M., and Zhu, B.: Application of Argo Data in the Analysis of Water Masses in the Northwest Pacific Ocean, Mar. Sci. Bull., 10, 1–13, 2008.

Sun, J., Steindler, L., Thrash, J. C., Halsey, K. H., Smith, D. P., Carter, A. E., Landry, Z. C., and Giovannoni, S. J.: One carbon metabolism in SAR11 pelagic marine bacteria, PLoS One., 6, e23973, https://doi.org/10.1371/journal.pone.0023973, 2011.

Tanioka, T. and Matsumoto, K.: Stability of Marine Organic Matter Respiration Stoichiometry, Geophys. Res. Lett., 47, e2019GL085564, https://doi.org/10.1029/2019gl085564, 2020.

Tian, D.: Stoichiometric deviation and regulatory mechanisms of AOU–nutrient ratio in the oligotrophic Northwest Pacific Ocean, Figshare [data set], https://doi.org/10.6084/m9.figshare.31841125, 2026.

Tian, D., Li, X., Song, J., Ma, J., Yuan, H., and Duan, L.: Biogeochemical layering and transformation of particulate organic carbon in the Tropical Northwestern Pacific Ocean inferred from δ13C, Ocean Sci., 21, 1627–1639, https://doi.org/10.5194/os-21-1627-2025, 2025.

Tréguer, P. J. and De La Rocha, C. L.: The world ocean silica cycle, Ann. Rev. Mar. Sci., 5, 477–501, https://doi.org/10.1146/annurev-marine-121211-172346, 2013.

Wan, X. S., Sheng, H.-X., Liu, L., Shen, H., Tang, W., Zou, W., Xu, M. N., Zheng, Z., Tan, E., Chen, M., Zhang, Y., Ward, B. B., and Kao, S.-J.: Particle-associated denitrification is the primary source of N_2O in oxic coastal waters, Nat. Commun., 14, 8280, https://doi.org/10.1038/s41467-023-43997-3, 2023.

Yu, X., Zhuang, Y., Cai, X., and Qi, D.: Role of Marginal Seas in Deep Ocean Regeneration of Dissolved Silica: A Case Study in the Marginal Seas of the Western Pacific, Front. Mar. Sci, 9, 925919, https://doi.org/10.3389/fmars.2022.925919, 2022.

Zhu, Z., Song, G., Zhang, Z., Luo, Y., Liu, S., and Zhang, J.: On the Stoichiometry of Degradable Fraction of Particulate Organic Matter Along a Diapycnal Mixing Path Using Dissolved Oxygen δ^{18}O Approach, J. Geophys. Res.-Oceans., 130, e2025JC022512, https://doi.org/10.1029/2025jc022512, 2025.